



Accumulation, transformation and transport of microplastics in estuarine fronts

This is the peer reviewed version of the following article:

Original:

Wang, T., Zhao, S., Zhu, L., Mcwilliams, J.C., Galgani, L., Amin, R.M., et al. (2022). Accumulation, transformation and transport of microplastics in estuarine fronts. NATURE REVIEWS. EARTH & ENVIRONMENT, 3(11), 795-805 [10.1038/s43017-022-00349-x].

Availability:

This version is available <http://hdl.handle.net/11365/1221378> since 2022-11-30T19:10:57Z

Published:

DOI: <http://doi.org/10.1038/s43017-022-00349-x>

Terms of use:

Open Access

The terms and conditions for the reuse of this version of the manuscript are specified in the publishing policy. Works made available under a Creative Commons license can be used according to the terms and conditions of said license.

For all terms of use and more information see the publisher's website.

(Article begins on next page)

1 *This version of the article has been accepted for publication, after peer review and is subject to*
2 *Springer Nature's AM terms of use, but is not the Version of Record and does not reflect post-*
3 *acceptance improvements, or any corrections. The Version of Record is available online at:*
4 <http://dx.doi.org/10.1038/s43017-022-00349-x>

5 *Wang, T., Zhao, S., Zhu, L. et al. "Accumulation, transformation and transport of microplastics in*
6 *estuarine fronts". *Nat Rev Earth Environ* 3, 795–805 (2022).*
7 *Available on the Publisher's website at this link <https://rdcu.be/cZJrJ>*

9 **Accumulation and Transformation of Microplastics in Estuarine Fronts**

11 Tao Wang^{1*}, Lixin Zhu², James C. McWilliams³, Luisa Galgani^{4,5}, Roswati Md Amin⁶, Ryota
12 Nakajima⁷, Wensheng Jiang¹, Mengli Chen⁸, Shiye Zhao^{7*†}

14 ¹Key Laboratory of Marine Environment and Ecology, Ocean University of China, Qingdao, China

15 ²Department of Marine and Environmental Science, Northeastern University, Massachusetts, USA

16 ³Department of Atmospheric and Oceanic Sciences, University of California, Los Angeles, Los
17 Angeles, California, USA

18 ⁴Harbor Branch Oceanographic Institute, Florida Atlantic University, Fort Pierce, Florida, USA

19 ⁵GEOMAR Helmholtz Centre for Ocean Research, Kiel, Germany

20 ⁶Faculty of Science and Marine Environment, Universiti Malaysia Terengganu, Kuala Nerus,
21 Malaysia

22 ⁷Japan Agency for Marine-Earth Science and Technology, Yokosuka, Japan

23 ⁸Tropical Marine Science Institute, National University of Singapore, Singapore

25 *These authors contributed equally to this work.

26 †Corresponding author: szhao@jamstec.go.jp

29 **Abstract**

31 Million tons of riverine plastic waste, numerically dominated by microplastics, annually enter the
32 ocean via estuaries. Featured by strong horizontal convergence, estuarine fronts, ubiquitous coastal
33 features, plausibly accumulate, transform and further involve microplastics into diverse processes,
34 but have received limited attention. In this Perspective, we discuss the accumulation potential of
35 microplastics and its subsequent interactions with physical-biological-geochemical processes at
36 estuarine fronts. Microplastics fragmentation and transformation could be enhanced within frontal
37 systems due to strong turbulence and interactions with sediment and biological particles, thus
38 intensifying potential impacts on ecological and biogeochemical processes. The concurrent
39 accumulation of microplastics and biota at fronts provides a unique chance to assess microplastics
40 risks at high concentrations, a likely common scenario in future ocean. Transdisciplinary efforts
41 in the mechanics of plastic dispersal, accumulation and fate in frontal zones will advance the
42 knowledge of riverine microplastics fate, favoring the developments of mitigation policies,
43 strategies and techniques.

45 **Introduction**

46
47 In 2016, an estimated 19–23 million metric tons (MT) of land-based mismanaged plastic waste
48 entered aquatic ecosystems worldwide¹. In the environment, plastic debris break into smaller
49 pieces termed microplastics (<5 mm) via natural fragmentation processes². Microplastics, coming
50 in different sizes, shapes, colors and chemical matrices³, dominate the number of plastic debris
51 and represent a planetary threat to Earth system⁴. As plastic load into natural environments will
52 raise in next few decades⁵, their continuous fragmentation will inevitably lead to an elevated
53 exposure of aquatic organisms to microplastics and associated chemicals. It was projected that 91%
54 of mismanaged plastic waste generated globally was transported via watersheds (>100 km²,
55 suggesting rivers as major pathways for plastics to the ocean⁶. A critical estimate of the annual
56 riverine plastic loads into the global ocean is 0.8 to 2.7 million MT⁷, roughly representing up to
57 50% of land-based plastic emissions (4.8–12.7 million MT)⁸.

58
59 Upon reaching estuaries, microplastics, like well-studied suspended particles, are fractionated by
60 physical, geochemical, biological, and ecological processes, and these dynamics potentially
61 determine the fate of plastics⁹⁻¹¹. One important hydrological feature in estuarine system is the
62 formation of density fronts when two distinct water masses interact and present sharp density
63 transitions^{12,13}. In general, density fronts occur throughout the ocean at different spatial and
64 temporal scales and are generally active in that there are a convergent flow and vertical
65 circulations^{12,14-16}. Their most immediate environmental effect is the occurrence of poor water
66 quality due to the frontal circulation converging flotsam, toxins, and organisms¹⁷⁻²⁰. Frontal
67 accumulation of pollutants is of functional importance in the dispersion of oceanic pollutants. For
68 instance, the enhanced aggregation of surface drifters by fronts in the Gulf of Mexico indicates
69 that the convergence associated with fronts is efficient in accumulating floating pollutants, thereby
70 possibly facilitating cleanup²¹. Compared to the submesoscale fronts in the open ocean, estuarine
71 fronts usually exhibit considerably stronger horizontal convergence²²⁻²⁴, vertical velocities^{25,26},
72 and turbulent mixing²⁷⁻²⁹ (FIG. 1), plausibly resulting in stronger convergences of flotsam and
73 various types of organisms^{30,31}. These, in turn, have major implications for the
74 biological, ecological, and biogeochemical health of the estuarine ecosystem^{13,32}. Although some
75 observations suggest that estuarine fronts have potential influences on the redistribution and fate
76 of riverine plastics^{31,33-35}, these impacts, especially on microplastics, have not yet received
77 sufficient attention³⁶⁻³⁸.

78
79 The aim of this Perspective is to illustrate the potential effects of estuarine surface fronts on the
80 accumulation, transformation and transportation of microplastics by combining insights from
81 hydrology, biology, ecology and geochemistry. We also propose that plastic hotspots at estuarine
82 fronts provide opportunities for the development and mobilization of mitigation strategies and
83 collection technologies to offset riverine plastic emissions, complementing existing approaches.
84 Finally, we suggest knowledge gaps that shall be addressed in future work to develop a better
85 mechanistic understanding of how microplastics behave in estuarine frontal systems.

86 **Main types of estuarine fronts**

87 Due to the interaction between buoyant freshwater and dense seawater, estuaries exhibit large
88 salinity variance and the strongest density fronts of any marine environment^{12,39}. Estuarine surface
89 fronts have apparent surface features allowing for easy observations of pollutant accumulation^{13,40};

90 therefore, this type of fronts is emphasized in this perspective. Bottom fronts are not discussed
91 here since they are not as easily observed as the surface fronts. However, they also have potentially
92 important effects on riverine plastics^{35,41}.

93 Three most common surface fronts in estuarine systems are considered: shear fronts, tidal intrusion
94 fronts and plume fronts (FIG. 2). These types of fronts are not mutually independent. For instance,
95 shear fronts can produce buoyancy-driven flow structures that propagate away from the generation
96 region as plume fronts¹².

97 **Shear fronts.** As one kind of the most common fronts inside the estuary⁴⁰, shear fronts are usually
98 aligned longitudinally and located at the inner edge of the shoals⁴², over the main channel⁴³ or
99 behind headlands and islands⁴⁴ (FIG. 2a). They might extend for several kilometers and exist for
100 several hours in one tidal cycle. Shear fronts are often triggered by the cross-channel shear of
101 surface longitudinal tidal currents in the regions with sharp depth gradients or behind headlands
102 and islands, and develop through flow convergences^{24,44} (FIG. 2a,b). The well-known axial
103 convergence front is one particular case of shear fronts because it is triggered by the transverse
104 shear of tidal currents⁴³. Although termed as “shear front”, some other mechanisms might also
105 contribute to the frontogenesis, such as confluence⁴⁵, convergence²⁴ and heterogeneous cross-
106 channel distribution of tidal mixing⁴⁶.

107 **Tidal intrusion fronts.** Tidal intrusion fronts are often formed when denser coastal waters plunge
108 beneath lighter estuarine waters during a flood tide into the constricted estuary mouth⁴⁷ (FIG. 2a,c).
109 Intrusion fronts will be evident in estuaries where incoming tidal water masses prevail over river
110 discharge. They are particularly pervasive in small estuaries around the world and usually marked
111 by a pronounced ‘V’ shape⁴⁸ (FIG. 2a). In addition to the estuarine mouth, tidal intrusion fronts
112 can also occur when tidal currents flow across constricted topographies inside the estuary⁴⁹.

113 **Plume fronts.** A river plume is formed when freshwater of riverine origin spreads over the coastal
114 water. As the plume spreads offshore, it creates one or several clear frontal boundaries onto the
115 continental shelf between the river plume and neighboring marine waters (FIG. 2a,d). These
116 boundaries with high horizontal density gradients are termed as plume fronts (FIG. 2d). The
117 locations of plume fronts vary in different estuarine systems, which mainly depend on the
118 extension and pathway of the diluted water as well as some local frontogenetic mechanisms⁵⁰. The
119 triggering mechanisms for the plume frontogenesis include the flow separation at the jetty of the
120 estuarine mouth due to cross flow⁵¹, hydraulic response to flow over the shoal⁵⁰, the seaward
121 advection of the tidal intrusion front¹³, and the interactions between the coastal and plume
122 currents¹⁶.

123 Overall, all three types of fronts usually exhibit strong surface convergence, downwelling and
124 turbulence (FIG. 1). In a realistic front, frontogenesis is the result of several mechanisms rather
125 than just one. Despite complex dynamics, the three types of surface fronts are often visually
126 observable as well as detectable through satellite images due to watercolor differences and
127 accumulations of foam and debris (FIG. 2b,c,d). Since their occurrence is related to periodical tidal
128 currents and topographies, their approximate occurrence locations and times in an estuary are
129 predictable from the observations of river discharge, tidal currents, and topography. The prediction
130 of a more precise occurrence time and location of estuarine fronts often requires high-resolution

131 numerical modellings^{16,52,53}, because aperiodic forcings, such as river discharge and winds can
132 influence the generation and movement of some fronts.

133 **Microplastic accumulation**

134 Various frontal processes spanning from the coast to the open ocean are thought able to cause
135 surface convergence, trap and retain plastic debris⁵⁴⁻⁵⁶. By converging plastic debris, fronts might
136 offer an opportunity for focused cleanup actions in the ocean^{55,57}. The differences in microplastics
137 abundances between open-ocean frontal and ambient waters demonstrate the marked convergence
138 effects along the fronts (meso⁵⁸ and submeso-scale⁵⁹⁻⁶¹) (FIG. 1b). Despite this fact, convergent
139 features accumulating floating plastics are rarely studied in the open ocean⁵⁵, and the investigation
140 of estuarine fronts on retaining plastics is even fewer. Nevertheless, the existing studies clearly
141 identify the enrichment of microplastics at fronts compared to ambient waters³⁶⁻³⁸ (FIG. 1b).
142 Meanwhile, we must note that microplastics abundances (300-5000 μm ; 89-2200 pieces/ m^3) at
143 estuarine fronts, standardized with methods in literature^{62,63}, are remarkably higher than those (1.4-
144 123.2 pieces/ m^3) observed in the open-ocean fronts, and larger than the maximum value observed
145 within the Great Pacific Garbage Patch (9.0 pieces/ m^3 ; FIG. 1b)⁶⁴, believed to hold the greatest
146 concentration of floating plastics of all ocean gyres⁶⁵. Modelling studies also demonstrated the
147 occurrence of microplastics hotspots along salinity fronts^{66,67}. Additionally, some other studies
148 ascribed the observed distribution patterns of microplastics to the estuarine salinity fronts^{31,33,34}.
149 All these preliminary evidences strongly suggest that estuarine fronts, as transition zones between
150 the input sources of land-based plastic debris and the open ocean have the capacity to accumulate
151 extraordinarily high loads of plastics. Compared to the inner shelf and open-ocean fronts, the
152 recurrent estuarine fronts establish more rapidly and are predicted with confidence in time and
153 space¹⁹. Furthermore, estuarine fronts are geographically and temporally accessible and are easily
154 recognized by environmental practitioners with a trained eye because of the accumulation of foam
155 and flotsam and the contrasting watercolor and clarity (FIG. 2). The recurrent and cumulative
156 features of estuarine fronts are important to retain riverine floating materials, and consequently
157 highlight their central role in intercepting and accumulating plastic debris. Although not detailed
158 in this context, we must note that the estuarine bottom fronts are also efficient in trapping and
159 concentrating riverine macro-plastic debris^{35,41}.

160 **Microplastic transformation**

161 Due to the characteristic flow convergence, floating materials are retained at fronts where the
162 matching of physical, biological and geochemical time-space scales provides the potential to
163 greatly modify the properties of suspended materials from rivers to the ocean^{48,68} (FIG. 3).
164 Microplastics incubated in this complex reactor can be subject to major alternations (fragmentation
165 and aggregation, FIG. 3b,c,d), largely determining their environmental fate and effects.

166 **Fragmentation.** In the natural environment, plastics become brittle and fragment into smaller
167 pieces under different weathering processes including photodegradation, biodegradation, thermal
168 degradation, mechanical destruction and hydrolysis, of which photodegradation is the only notable
169 mechanism leading to rapid environmental degradation of plastic polymers². Exposure of plastic
170 to ultraviolet (UV) radiation is the critical step to initiate autocatalytic thermal oxidation that
171 principally accounts for their subsequent fragmentation⁶⁹. Once initiated, oxidation reactions could

172 result in the bulk fragmentation of plastics yielding large daughter fragments; at the same time, the
173 surface-ablation fragmentation of plastics, which releases large amounts of microscale plastics
174 from UV-facilitated brittle surface layer, will progress along with the bulk fragmentation. The
175 mechanical forces such as sand grinding, collision and interaction with biotic particles, wave and
176 wind actions, can disintegrate and detach the weathered surface layer into micro- and nanoplastics
177 through the abrasion wear^{69,70}. Both field and laboratory data indicated that the surface-ablative
178 fragmentation is primarily responsible for most of secondary microplastics in the environment<sup>71-
179 75</sup>. In rivers and estuaries, microplastics at different states of degradation were widely identified,
180 manifested by obvious rough surface textures (for instance, pits, fractures and flakes) and
181 discoloration⁷⁶⁻⁷⁹. The wear of photo-oxidated plastics against erosive sand can efficiently generate
182 smaller fragments, likely dominated by particles smaller than 100 μm ⁷³. After 500 hours of
183 exposure in the UV light chamber, polypropylene plastics incubated in seawater showed strong
184 degradation (cracks and holes) on their surfaces with missing small pieces of material in the sub-
185 micron range⁷⁵. This result was attributed to the combined action of UV radiation and wave action,
186 and the missing fragments accounted for an average 0.1% of the initial plastic weight. To better
187 understand this surface-ablation mode of fragmentation, we calculated the theoretical amount of
188 100 nm and 1 μm cubic particles generated from the weight loss of polypropylene plastics in REF⁷⁵.
189 The 0.1% of weight loss approximately equals to 10^{18} and 10^9 pieces of 100 nm and 1 μm particles,
190 respectively, corresponding to 2×10^{16} pieces/liter and 2×10^7 pieces/liter. These large numbers
191 of secondary fragments from the surface-ablation fragmentation might represent a pressing health
192 concern for aquatic biota. The frontal zone is well known as an effective trap of the river-laden
193 sediments (for example, the concentration could be up to 10 g/L in the Amazon frontal zone⁸⁰) and
194 biological particles^{12,19}. Additionally, the turbulent kinetic energy dissipation rate could be about
195 1–2 orders of magnitude greater along estuarine fronts than in the surrounding waters (FIG. 1a).
196 Due to the stronger turbulent energy and higher concentrations of suspended particles at fronts
197 with respect to ambient conditions, the encounter kernel rate (Collision Frequency) of suspended
198 particles will substantially increase in estuarine frontal zones⁸¹⁻⁸⁵ (BOX 1). Therefore, the presence
199 of single or combined factors (high concentrations of particles and strong turbulence) in the frontal
200 zones will considerably increase the probability of the surface-ablative fragmentation of UV-
201 weathered plastic debris (FIG. 3b). However, the surface-ablation mode of fragmentation in
202 aquatic environments is not yet sufficiently understood^{74,75,86-88}, and further data are required to
203 disclose the detailed dynamics of this process.

204
205 **Aggregation.** Besides the transport process facilitating particle collisions (BOX 1), destabilization
206 with reducing interparticle repulsion also controls particle aggregation⁸⁹. Although the
207 destabilization mechanisms are initially assumed to cover small-sized particles (<1 μm), they also
208 apply to the aggregation processes of millimeter-sized particles⁸¹. Upon entering rivers, particles
209 are immediately coated with natural organic matter (mainly carboxyl and phenolic-OH⁹⁰)
210 producing a uniformly negative surface charge¹⁰. The negative charge on the particle-organic
211 matter surface creates an electrostatic ‘double layer’, whose distance determines the range of
212 interparticle repulsive forces and restricts particle aggregation⁸¹. As approaching the estuaries,
213 counter ions (especially cations Ca^{2+} and Mg^{2+}) are attracted by electrostatic forces, which will
214 screen the electrostatic repulsive force and compress the distance of the double layer. The
215 compression of double layer allows the short-range attractive *van der Waals forces* to occur,
216 permitting particles to approach more closely^{10,81}. Due to the raising ionic strength, the
217 enhancement of river-borne particle aggregations in estuaries has been widely acknowledged^{10,91,92}.

218 Although the charge neutralization is the major destabilization process, some other mechanisms
219 also come into play: an example is the hydrophobic character of particles which provides
220 appreciable attraction between particles through the so-called 'hydrophobic bonding'⁸¹. The
221 resulting attractive force between particles and hydrophobic segments is unexpectedly large and
222 promotes considerable aggregation^{93,94}. The hydrophobic interaction is particularly true when
223 considering the higher hydrophobicity of plastic particles in the aquatic environment compared to
224 naturally suspended particles.

225 Apart from the physical and geochemical mechanisms of particles coagulation, biologically-
226 generated organic compounds like extracellular polymeric substances (EPS)⁹⁵, also play an
227 important role in holding the particles together^{85,96}. EPS exuded by phytoplankton and bacteria in
228 aquatic systems is constituted of sugars, proteins, nucleic acids and lipids. EPS also serves as the
229 biological glue which controls coagulation efficiencies and enhances the formation of particle
230 aggregations^{97,98}. The sticky nature of EPS is usually attributed to its polyanionic nature, such as
231 carboxylic and sulfate half-ester groups^{99,100}. For example, the stickiness of the diatom-derived
232 transparent exopolymer particles (TEP), one type of EPS, was observed as generally 2–4 orders of
233 magnitude higher than that of most other particles^{101,102}. Laboratory experiments showed that
234 biogenic particles could intensively interact with microplastics and generate more pronounced
235 aggregates and TEP with respect to treatments without plastic addition¹⁰³⁻¹⁰⁵. Furthermore, TEP
236 stickiness appears to increase along the salinity gradient, implying a seaward enhancement in
237 particle aggregation¹⁰⁶. The production of TEP could also be enhanced by high cell abundances¹⁰²
238 and high turbulence intensity¹⁰⁷. These evidences indicate that the secretion of EPS by
239 microorganisms in estuarine fronts could be particularly elevated. For instance, TEP from
240 organisms at fronts created mucilaginous foams and gels at the water surface¹⁰⁸, and condensed
241 gelatinous aggregates along frontal systems were observed in the northern Adriatic Sea¹⁰⁹.
242 Additionally, particles can be ingested by organisms and expelled in their feces or pseudo-
243 feces^{110,111}. The bio-deposits of many aquatic animals are generally mucus-bounded¹¹² and can
244 trap other particles, further aggregating riverine particles¹¹³. These biogenic compounds determine
245 the stability and particle size of aggregates and thus are essential to maintain the steady-state
246 population of aggregate sizes in the presence of the turbulent forces¹¹⁴. The high abundance of
247 organisms and biological activities, combined with the increased particle collision frequency due
248 to turbulent forces (BOX 1) and geochemical conditions at estuarine fronts, will enhance the
249 aggregation of microplastics (FIG. 3d).

250 **Microplastic transport**

251 Once plastics are entrapped in the frontal systems, transport mechanisms become more complex
252 because numerous physical and biological processes interact as waters of different densities come
253 into contact¹⁹. Considering the enhanced cross-frontal vertical circulations and biological factors,
254 a marked three-dimensional transport of microplastics might be expected at the front.

255 **Physical transport.** Horizontally, fronts generally tend to converge materials in the cross-front
256 direction and transport them mainly in the along-front direction¹⁵. Once fronts fragment or
257 dissipate, the convergent materials (including microplastics) are likely dispersed into the
258 surrounding waters, resulting in a single large pulse of plastic⁶⁸. Vertically, estuarine fronts usually
259 feature strong downwelling velocities and turbulent mixing (FIG. 1a). Results from models have

260 clarified that strong downwelling currents and turbulence at fronts can subduct surface particles
261 into the water column^{116,117} (FIG. 3a). In combination with the enhanced aggregation, the sinking
262 rates of microplastics in frontal zones will considerably increase, speeding up their removal from
263 the surface. Experiments and field observations demonstrate that aggregates are an efficient vector
264 for vertical transport of microplastics in the water column through increasing settling velocities by
265 orders of magnitudes^{105,118-120}. Lastly, smaller microplastics trapped in mucilaginous foams along
266 the fronts might be lifted into the air by breaking waves and winds. Although studies in this respect
267 are limited, both microplastic fragments ($\leq 300 \mu\text{m}$) and microfibers (up to $750 \mu\text{m}$) have been
268 widely detected in the wet¹²¹⁻¹²⁴ and dry atmospheric depositions, suggesting longer-range
269 transport¹²⁵. Furthermore, models and observations agree in the possible transfer of microplastics
270 from surface seawater to atmospheric aerosols through wind and wave actions¹²⁶⁻¹²⁸, substantially
271 contributing to the atmospheric microplastics load. As such, 11% of atmospheric microplastics in
272 the western United States derive from the secondary re-emission of floating plastic marine
273 debris¹²⁸. These evidences suggest that microplastics accumulation zones in aquatic environments
274 represent important potential sources of atmospheric microplastics, and this particularly applies to
275 the 3-D transport of microplastics at fronts.

276
277 **Bio-transport.** The elevated plankton biomass in estuarine fronts creates feeding “hotspots” for
278 planktivorous fishes (for example anchovy, herring and juvenile salmonids), which subsequently
279 attract piscivorous fishes, birds, and mammals and enhance the energy and pollutants transfer to
280 higher trophic levels^{129,130}. If the swimming speeds of these organisms overcome the convergent
281 current velocity, the advection and diffusion of organisms as well as the associated pollutants are
282 likely to occur¹³¹. The bio-transport of persistent organic pollutants (POPs), such as
283 polychlorinated biphenyls and dichlorodiphenyltrichloroethane in migrating birds, marine
284 mammals and fishes has been observed¹³²⁻¹³⁴. It is therefore expected that microplastics could
285 experience a similar transport pattern via being mistaken by or attached to aquatic organisms in
286 fronts (like seaward juvenile salmonids and seabirds^{130,135}) (FIG. 3a).

287
288 **Modelling microplastic transport.** Numerical modeling is one of the most effective tools to
289 simulate and study estuarine fronts and microplastics transport. Although the number of
290 observations of estuarine surface fronts has massively increased since the 1970s (REFS^{12,13,19,40}),
291 numerical simulations in realistic estuaries only concentrate in the 21st century, benefiting from
292 the increasing resolution and performance of three-dimensional baroclinic hydrodynamic models.
293 To date, some numerical models have been applied successfully in a few estuaries to simulate
294 frontal dynamics, including the occurrence time and locations of fronts, frontogenesis, three-
295 dimensional velocities at fronts and frontal instabilities (Supplementary Table 1). Based on the
296 hydrodynamic fields generated from these models, the transport and fate of microplastics in
297 estuaries can be further simulated, and thus help predict microplastics hotspots^{66,67}.

298
299 Numerical simulations of the transport and fate of microplastics in the coastal and open ocean were
300 generally carried out based on the Eulerian or Lagrangian frameworks. In the Lagrangian
301 framework, microplastics are represented by individual virtual particles, which are allowed to
302 move through the time-evolving velocity fields^{136,137}. The effect of turbulence is sometimes
303 included as ad hoc random motions^{137,138}. In addition to the extensive applied Lagrangian particle-
304 tracking oceanic models summarized in REF¹³⁷, some other particle-tracking models have also
305 been applied to microplastic transport simulations in coastal and estuarine regions, for instance the

306 three dimensional hydrodynamic and suspended sediment transport model (HYDROTAM-3D)¹³⁹,
307 Track Marine Plastic Debris (TrackMPD)¹⁴⁰, Delft3D-Water Quality Particle tracking module (D-
308 WAQ PART)¹⁴¹, and Ichthyoplankton (Ichthyop)¹⁴². Unlike the Lagrangian approach, Eulerian
309 models simulate microplastics as passive tracers in terms of their mass or volume concentrations,
310 which are advected by the velocity fields and diffused by the parameterized turbulence⁶⁷.

311
312 Besides the hydrodynamic fields, which are considered in the common oceanic particle-tracking
313 models, some other important factors also have effects on microplastics movements, such as the
314 physical properties of plastic particles (density, shape, size), windage, beaching, sedimentation,
315 resuspension, fragmentation, biofouling, and ingestion by animals. As an example, the difference
316 between the densities of plastic particles and ambient waters affects the vertical movements of
317 microplastics¹⁴³, whereas the fragmentation-facilitated decrease in particle size and biofouling
318 influence plastic transport^{144,145}. Therefore, modeling the transport trajectories of oceanic
319 microplastics is challenging and all of the current numerical models employ certain simplifying
320 assumptions. Two most frequently used assumptions are considering microplastics as positively
321 buoyant particles and tracking microplastics under the effects of ocean surface currents, without
322 including additional mechanisms of sinking, ingestion or other removal from the ocean surface.
323 Such simplified models have been strikingly successful in explaining the hotspots of microplastics
324 in the coastal- and open-ocean surface waters^{66,146,147}. However, there is still a large gap between
325 masses of floating plastics in the ocean and the land-based fluxes of plastic debris to the ocean,
326 sparking discussions about “missing plastics”^{8,148,149}. To better understand the final sinks of these
327 “missing plastics”, some modeling efforts have also simulated or parameterized more mechanisms,
328 including the vertical movement due to buoyancy¹⁴³ and mixing¹³⁸, beaching and re-
329 suspension^{150,151}, sedimentation¹⁵², fragmentation¹⁵³, and biofouling^{144,154}.

330
331 As stated above, although the accuracies of the hydrodynamic and plastic-tracking models are
332 waiting for future improvements, their successful applications in previous studies have shed light
333 on microplastic dynamics at estuarine fronts. By simulating estuarine dynamics and microplastic
334 transport, Cohan et al. (2019)⁶⁶ and Bermurdez et al. (2021)⁶⁷ found that microplastics accumulate
335 at the fronts of the Delaware and Guadalquivir estuaries, respectively. With the development of
336 the hydrodynamic and microplastic-tracking models, the simulations of microplastic dynamics in
337 estuaries are worthy of efforts, especially the processes related to accumulation, redistribution and
338 residence time at fronts.

339 340 **Ecological impacts**

341 The concurrence of pollutants and organisms at fronts through advectively-imposed matching or
342 behavioral movement inevitably threatens the estuarine ecosystem health and biogeochemical
343 processes^{18,19}. High levels of microplastics at fronts resulting from convergent circulations are
344 likely common in the future as the annual plastic waste entering aquatic ecosystems is expected to
345 increase in the coming decades^{5,155}. Therefore, estuarine frontal regions are key environments,
346 where the understanding of the ecological consequences of microplastics is critical to develop
347 ecological and biogeochemical models for future predictions.

348 **Ecotoxicological risk.** Biological enrichment at estuarine fronts is prevalent in a wide range of
349 neuston and planktonic organisms, such as phytoplankton, planktonic copepods, fish eggs, larval

350 fishes and insects^{131,156}. The concentrated biomass coupled to high abundances of microplastics
351 raises the probability of encounter and ingestion of microplastics for aquatic organisms in frontal
352 zones. Gove et al. (2019)⁵⁹ found that the plastic-to-larval fish ratio (7:1) in the coastal ocean
353 convergence along the coast of Hawaii Island was 14 times that in the ambient waters. Moreover,
354 they identified that plastic ingestion by larval fishes in the oceanic fronts was 2.3-fold higher than
355 in ambient waters. Compared to adult fishes, larval fishes were more vulnerable to the consequence
356 of microplastics ingestion because of their underdeveloped organs¹⁵⁷. A wide range of aquatic
357 organisms at the bottom of the food chain can ingest microplastics^{158,159}, showing a positive
358 correlation between the bio-uptake rates and microplastics abundances^{160,161}. Microplastics can
359 substitute the food in the diets of zooplankton and thus decrease their natural food consumption,
360 subsequently lowering the carbon export efficiency through an impaired fecal pellet sinking rates
361 and the biological pump^{120,162}. Smaller microparticles (<150 µm) can translocate across biological
362 membranes and become entrapped in organisms' tissues, potentially leading to bioaccumulation
363 and biomagnification through the entire food web^{4,163}. Small sized particles can also accelerate the
364 release of chemicals inherent in plastic polymers (for instance, carbon and additives)¹⁶⁴. Some
365 contrasting evidences exist as well: one research in the Cooper River, USA found no statistically
366 significant differences in microplastic consumption by zooplankton at the tidal fronts and in the
367 surrounding waters, although higher abundances of microplastics were identified at the front³⁶.
368 Low grazing rates of microplastics by zooplankton were also observed in laboratory assays that
369 typically employ higher plastic concentrations^{165,166}, which was largely ascribed to the animal
370 selective feeding behavior. Altogether, these findings suggest that microplastics consumption is a
371 function of plastic abundances as well as size and shape, while other factors related to plastics
372 (such as biofouling, aggregation, chemical sorption and release), and the aquatic biota feeding
373 mechanisms, also play a key role¹⁶⁷⁻¹⁷⁰. In frontal systems, the synergic effects of high particles
374 abundances, small particle size, enhanced plastic incorporation into biological aggregates
375 expectedly increase microplastics bioavailability. This higher bioavailability can enhance the
376 accessibility of smaller microplastics to biological tissues, accelerate additive leaching rates, and
377 consequently expose different trophic organisms in frontal habitats to the threats of plastic
378 pollution⁴. The shorter and more efficient path length of food webs in frontal systems¹⁷¹ has a
379 great potential to rapidly channel a sufficient proportion of ingested microplastics to higher trophic
380 levels. Besides resulting in the elevated ratio of microplastic-to-prey particles, the convergence of
381 both plastic and biological particles at fronts also has the potential to dilute the concentrations of
382 microplastics, hence making microplastic bioavailability become more difficult to model and
383 deserving further attention, since microplastic dilution in frontal systems has not been verified yet.

384 **Biogeochemical influences.** Aside from increased ecotoxicological threats through microplastics
385 ingestion, the accumulation of these particles at fronts can also impose substantial impacts on
386 biogeochemical elements' cycling. Enhanced particle fragmentation and strong turbulence in
387 frontal regions, as well as photo-oxidation, can increase the leaching rate of plastic-related
388 chemicals through the deterioration and disruption of polymeric structures^{164,172}. The leaching rate
389 of one-half additives from a plastic fragment increases exponentially with a decrease in size¹⁶⁴.
390 Under controlled turbulent conditions, leaching rates of additives and polymer oligomers from
391 microplastics are considerably enhanced. In these settings, the rate of chemical release from
392 microplastics in turbulent conditions can be up to 190-fold higher than that from plastics in the
393 non-turbulent conditions¹⁷². Therefore, the leaching of both fossil-based carbon in the polymer
394 backbone^{173,174} and chemical additives (at least 906 different types¹⁷⁵) could be speeded up in

395 estuarine frontal environments. Controlled experiments documented that microplastic leachates
396 apparently changed the microbial communities and nitrogen cycling processes by transforming
397 metabolic intermediates and enzymes activities of microbes^{176,177}. Furthermore, the enhanced
398 microplastics ingestion in frontal systems could potentially change the water biogeochemistry. It
399 was predicted that consumption of microplastics by zooplankton in the open ocean could reduce
400 the grazing on phytoplankton and thus result in the elevated organic carbon export, which upon
401 remineralization decreases the oxygen and returns nutrients to the water column¹⁷⁸. Zobell (1943)
402 found that trace nutrients could concentrate on solid surfaces in the water column, thereby
403 becoming more bioavailable and stimulating bacterial respiration¹⁷⁹. Elevated nutrients on plastic
404 surface can strengthen the metabolism and interactions of both autotrophic and heterotrophic
405 bacteria and enhance the production of EPS and the formation of particulate aggregates^{104,180}.
406 Similar to what has been proposed for the open ocean¹⁷⁸, predictably increased consumption of
407 microplastics by zooplankton might also accelerating deoxygenation of these environments¹⁷⁸. In
408 shallow estuarine systems, a rapid aggregation and consequent sedimentation of microplastics
409 embedded into biogenic material can enhance benthic oxygen respiration creating anoxic
410 sediments conditions; this process can have large impacts on coastal nutrient cycling and large-
411 scale geochemical dynamics that involve chemical exchanges at the interface between seawater
412 and sediments.

413

414 **Implications for pollution mitigation**

415 Based on a high-resolution global map showing the probability for land-based plastics to enter the
416 ocean, Meijer et al. (2021) predicted an annual flux of riverine plastic ranging from 0.8 to 2.7 MT⁷.
417 Contrary to previous estimates, those reported a few large rivers (47 and 5 rivers^{181,182}) holding
418 responsible for the vast majority of annual plastic load to the ocean, the results by Meijer and
419 colleagues showed that 1656 rivers accounted for 80% of the global plastic emissions. Of these
420 1656 rivers, small and medium-sized rivers contributed 96% of the plastic load, whereas large
421 rivers made up only 4.0%. The urban rivers in South East Asia and West Africa were identified as
422 the principal contributors⁷. Understanding the mechanisms behind the transport and transformation
423 of plastics in estuaries is a prerequisite to inform environmental stakeholders and policy makers,
424 and for developing efficient solutions at or near the source of these debris before they reach the
425 oceanic environment. However, progress-based observations of plastics in rivers and estuaries are
426 still few^{183,184}. Furthermore, there is an uneven distribution of studies on the world's estuarine
427 fronts and the rivers presumably responsible for the majority of the plastic load into the world's
428 ocean⁷. To date, knowledge on estuarine fronts is mostly derived from studies in North America
429 and Europe, where rivers' contribution to the global plastic export is limited (FIG. 4).
430 Contrastingly, estuarine fronts are largely understudied in Asia, where rivers account for the
431 majority (>60%) of the total flux of plastic debris into the ocean⁷. This mismatch impedes an
432 efficient control and mitigation of plastic pollution at these predicted hotspots, and indicates that
433 international collaboration and common agreements on plastic management are required¹⁸⁵.
434 Despite cross-border research on estuaries in Asia is still limited, it is encouraging to note that
435 some internal groups (for instance, the Ocean Cleanup and 'The National Geographic Society's
436 Sea to Source: Ganges Expedition') have started to study riverine plastics in these hotspots¹⁸⁶⁻¹⁹⁰.
437 In light of the substantial influence of estuarine fronts on riverine plastics, the hydrodynamics,
438 biological and geochemical processes at fronts merit in-depth investigation when monitoring
439 plastic pollution.

440

441 Simultaneously, lots of technologies such as net-based sampling, remote sensing, and camera
442 technologies have been developed to monitor and reduce plastic waste in global rivers¹⁸³. With
443 respect to riverine plastic cleanup, the implantation of different infrastructures in river channels to
444 extract plastic appear to be the most efficient approaches. For instance, floating booms (n=26)
445 were employed to collect debris in the Seine River in France¹⁹¹. In 2014, a trash interceptor driven
446 by the combination of solar and hydro power, known as Mr. Trash Wheel, was installed in the
447 Jones Falls¹⁹² (Maryland, USA) and has collected over 2000 tons of debris as of May 2022. By
448 employing a similar technique, the Ocean Cleanup advocated to tackle these 1000 most polluting
449 rivers. Estuarine fronts, as natural barriers for floating materials, can play a complementary role in
450 intercepting plastics in all size fractions before making their way into the ocean. The main types
451 of surface fronts are temporally recurrent, and easily predictable in time and space by making use
452 of available data of river discharge, tidal currents, topography and perfected by numerical
453 models. In the field, these fronts often show pronounced differences in watercolor, accumulations
454 of foam and debris (FIG. 2), and enhanced surface roughness which can be detected by ship-
455 mounted radars¹⁹³. Therefore, recovering plastics along estuarine fronts can be reasonably practical
456 and provide a complementary way to the currently available cleanup strategies, which can be more
457 efficient by coupling the newly affordable collection techniques such as unmanned aerial vehicles
458 (UAVs^{187,194,195}). For example, a specifically designed UAVs, automatically locating the recurrent
459 estuarine frontal zones, can be promising to leverage the plastic convergence at fronts and achieve
460 considerable recovery of plastic debris. Additionally, it must be noted that estuarine fronts are
461 regions of high ecological significance, where animals (adults and larvae) concentrate for
462 spawning, feeding and nursing¹⁹⁶. Sustainable strategies that minimally disturb ecosystems'
463 functioning are required to mitigate plastic pollution in frontal zones. As suggested in Sherman
464 and van Sebille (2016)¹⁹⁷, models that predict the dynamics of both plastics and marine life in
465 frontal systems, should be considered to guide the development and operation of clean-up
466 techniques and devices.

467 **Summary and future perspectives.** As the demand of plastic products increases, the riverine
468 plastic flux to the sea will likely follow this increasing pattern in the future^{1,155}. Despite substantial
469 progress in studying transport pathways and consequences of riverine plastics moving towards the
470 ocean, and in developing mitigation strategies and technological advancements¹⁸³, we still have a
471 vague understanding of most processes involving microplastics in estuarine fronts. Due to the
472 hydrodynamic, geochemical and biological characteristics of these estuarine fronts, we believe
473 that there is a reasonable scientific confidence that frontal systems could have considerable
474 influences on plastic transport, fate, and potential ecosystem impacts. The analysis in this
475 perspective suggests that microplastics and other particles could converge at estuarine fronts (FIG.
476 1 and FIG. 3ab), leading to an enhanced plastic fragmentation as well as leaching rate of chemicals
477 (FIG.3b and BOX 1). Furthermore, the concurrence of both microplastics and biotic particles
478 (phytoplankton, bacteria and TEP; FIG. 3b), would increase aggregates formation rates.
479 Microplastics transformations (fragmentation and aggregation) by frontal processes, together with
480 environmental (circulations and air-sea interactions) and ecological factors (bio-ingestion and
481 trophic transfer) ultimately facilitate the transport of microplastics and their integration into the
482 food web, posing physical and chemical threats to estuarine and coastal ecosystems. The recurrent
483 and predictable fronts in estuaries provide unique opportunities to mitigate riverine plastic
484 pollution and prevent plastic from reaching the ocean. We also suggest that estuarine fronts, where
485 high abundances of microplastics are similar to those expected in future ocean conditions (FIG.

486 1b), can be regarded as a natural laboratory setting to achieve a better understanding of future
487 microplastics impacts on marine ecosystem, providing the opportunity to act in time. Considering
488 the mismatch of the current knowledge on estuarine fronts and global riverine plastic emissions
489 (FIG. 4), new research efforts should converge different disciplines to investigate microplastics in
490 estuarine frontal zones and clarify their dispersal, fate and multifaceted interactions, aiding in
491 developing mitigation policies, techniques and strategies. Previous studies have individuated
492 essential research directions, crucial to a comprehensive understanding of the role of estuarine
493 fronts in plastic pollution, such as the prediction of plastic transport trajectories in the river-
494 estuary-sea continuum^{198,199}, plastic fragmentation¹⁸³, ecotoxicological effects (especially in
495 larvae)⁵⁹, and data standardization and sharing^{62,63}. Moreover, specific research topics that should
496 be prioritized also include the observation and accurate prediction of estuarine fronts (locations,
497 occurrence time and intensity), the converging capacity and turnover time of plastic debris in
498 different estuarine fronts, as well as the development of pollution mitigation strategies on the basis
499 of the hydrodynamic and biological characteristics of targeted environments. These actions we
500 propose herein are not exhaustive and many challenges still exist due to the extremely complexity
501 in both plastic debris composition and transformations, and estuarine processes. Nevertheless, we
502 hope that this paper contributes to raise worldwide attention on interactions between plastic debris
503 and physical-biological-geochemical mechanisms in frontal systems, and hopefully enables further
504 collaborative, interdisciplinary, and international efforts to limit plastic influx to the ocean and to
505 fill current knowledge gaps on wide-range environmental impacts of plastics.

506 References

- 507
- 508 1 Borrelle, S. B. et al. Predicted growth in plastic waste exceeds efforts to mitigate plastic
509 pollution. *Science* **369**, 1515–1518 (2020).
- 510 2 Andrady, A. L. Microplastics in the marine environment. *Mar. Pollut. Bull.* **62**, 1596–1605
511 (2011).
- 512 3 Rochman, C. M. et al. Rethinking microplastics as a diverse contaminant suite. *Environ.*
513 *Toxicol. Chem.* **38**, 703–711 (2019).
- 514 4 MacLeod, M., Arp, H. P. H., Tekman, M. B. & Jahnke, A. The global threat from plastic
515 pollution. *Science* **373**, 61–65 (2021).
- 516 5 Lau, W. W. et al. Evaluating scenarios toward zero plastic pollution. *Science* **369**, 1455–
517 1461 (2020).
- 518 6 Lebreton, L. & Andrady, A. Future scenarios of global plastic waste generation and
519 disposal. *Palgr. Commun.* **5**, 1–11 (2019).
- 520 7 Meijer, L. J., van Emmerik, T., van der Ent, R., Schmidt, C. & Lebreton, L. More than
521 1000 rivers account for 80% of global riverine plastic emissions into the ocean. *Sci. Adv.*
522 **7**, eaaz5803 (2021).
- 523 8 Jambeck, J. R. et al. Plastic waste inputs from land into the ocean. *Science* **347**, 768–771
524 (2015).
- 525 9 Zhang, H. Transport of microplastics in coastal seas. *Estuar. Coast. Shelf Sci.* **199**, 74–86
526 (2017).
- 527 10 Hunter, K. & Liss, P. The surface charge of suspended particles in estuarine and coastal
528 waters. *Nature* **282**, 823–825 (1979).
- 529 11 Mosley, L. M. & Liss, P. S. Particle aggregation, pH changes and metal behaviour during
530 estuarine mixing: Review and integration. *Mar. Freshw. Res.* **71**, 300–310 (2020).

531 12 O'Donnell, J. Surface fronts in estuaries: A review. *Estuaries* **16**, 12–39 (1993).
532 13 Uncles, R. in *Treatise on Estuarine and Coastal Science* (ed. Wolanski, E. & McLusky,
533 D.) 5–20 (2011).
534 14 McWilliams, J. C. Submesoscale currents in the ocean. *Proc. R. Soc. A Math. Phys. Eng.*
535 *Sci.* **472**, 20160117 (2016).
536 15 McWilliams, J. C. Oceanic frontogenesis. *Annu. Rev. Mar. Sci.* **13**, 227–253 (2021).
537 16 Wang, T., Barkan, R., McWilliams, J. C. & Molemaker, M. J. Structure of submesoscale
538 fronts of the Mississippi River plume. *J. Phys. Oceanogr.* **51**, 1113–1131 (2021).
539 17 Klemas, V. & Polis, D. A study of density fronts and their effects on coastal pollutants.
540 *Remote Sens. Environ.* **6**, 95–126 (1977).
541 18 Tanabe, S. et al. Persistent organochlorines in coastal fronts. *Mar. Pollut. Bull.* **22**, 344–
542 351 (1991).
543 19 Largier, J. L. Estuarine fronts: How important are they? *Estuaries* **16**, 1–11 (1993).
544 20 Poje, A. C. et al. Submesoscale dispersion in the vicinity of the Deepwater Horizon spill.
545 *Proc. Natl. Acad. Sci.* **111**, 12693–12698 (2014).
546 21 D'Asaro, E. A. et al. Ocean convergence and the dispersion of flotsam. *Proc. Natl. Acad.*
547 *Sci.* **115**, 1162–1167 (2018).
548 22 O'Donnell, J., Marmorino, G. O. & Trump, C. L. Convergence and downwelling at a river
549 plume front. *J. Phys. Oceanogr.* **28**, 1481–1495 (1998).
550 23 Marmorino, G. & Trump, C. Gravity current structure of the Chesapeake Bay outflow
551 plume. *J. Geophys. Res. Oceans* **105**, 28847–28861 (2000).
552 24 Collignon, A. G. & Stacey, M. T. Intratidal dynamics of fronts and lateral circulation at the
553 shoal-channel interface in a partially stratified estuary. *J. Phys. Oceanogr.* **42**, 869–883
554 (2012).
555 25 Mahadevan, A. The impact of submesoscale physics on primary productivity of plankton.
556 *Annu. Rev. Mar. Sci.* **8**, 161–184 (2016).
557 26 Orton, P. M. & Jay, D. A. Observations at the tidal plume front of a high-volume river
558 outflow. *Geophys. Res. Lett.* **32**, L11605 (2005).
559 27 D'Asaro, E., Lee, C., Rainville, L., Harcourt, R. & Thomas, L. Enhanced turbulence and
560 energy dissipation at ocean fronts. *Science* **332**, 318–322 (2011).
561 28 Yang, Y., San Liang, X., Qiu, B. & Chen, S. On the decadal variability of the eddy kinetic
562 energy in the Kuroshio Extension. *J. Phys. Oceanogr.* **47**, 1169–1187 (2017).
563 29 MacDonald, D. G. & Geyer, W. R. Turbulent energy production and entrainment at a
564 highly stratified estuarine front. *J. Geophys. Res. Oceans* **109**, C05004 (2004).
565 30 Acha, E. M., Mianzan, H. W., Guerrero, R. A., Favero, M. & Bava, J. Marine fronts at the
566 continental shelves of austral South America: Physical and ecological processes. *J. Mar.*
567 *Syst.* **44**, 83–105 (2004).
568 31 Hinojosa, I. A., Rivadeneira, M. M. & Thiel, M. Temporal and spatial distribution of
569 floating objects in coastal waters of central-southern Chile and Patagonian fjords. *Cont.*
570 *Shelf Res.* **31**, 172–186 (2011).
571 32 McCarthy, J. J., Robinson, A. R. & Rothchild, B. J. in *The Sea*, (ed. Robinson, A. R.
572 McCarthy, J. J. & Robinson, A. R.) Chapter 1 (John Wiley & Sons, 2002).
573 33 Rech, S. et al. Rivers as a source of marine litter—a study from the SE Pacific. *Mar. Pollut.*
574 *Bull.* **82**, 66–75 (2014).

- 575 34 Cheung, P. K., Cheung, L. T. O. & Fok, L. Seasonal variation in the abundance of marine
576 plastic debris in the estuary of a subtropical macro-scale drainage basin in South China.
577 *Sci. Total Environ.* **562**, 658–665 (2016).
- 578 35 Acha, E. M. et al. The role of the Río de la Plata bottom salinity front in accumulating
579 debris. *Mar. Pollut. Bull.* **46**, 197–202 (2003).
- 580 36 Payton, T. G., Beckingham, B. A. & Dustan, P. Microplastic exposure to zooplankton at
581 tidal fronts in Charleston Harbor, SC USA. *Estuar. Coast. Shelf Sci.* **232**, 106510 (2020).
- 582 37 Atwood, E. C. et al. Coastal accumulation of microplastic particles emitted from the Po
583 River, Northern Italy: Comparing remote sensing and hydrodynamic modelling with in situ
584 sample collections. *Mar. Pollut. Bull.* **138**, 561–574 (2019).
- 585 38 Pazos, R. S., Bauer, D. E. & Gómez, N. Microplastics integrating the coastal planktonic
586 community in the inner zone of the Río de la Plata estuary (South America). *Environ. Pollut.*
587 **243**, 134–142 (2018).
- 588 39 Geyer, W. & Ralston, D. Estuarine frontogenesis. *J. Phys. Oceanogr.* **45**, 546–561 (2015).
- 589 40 Brown, J., Turrell, W. & Simpson, J. Aerial surveys of axial convergent fronts in UK
590 estuaries and the implications for pollution. *Mar. Pollut. Bull.* **22**, 397–400 (1991).
- 591 41 Carman, V. G. et al. Young green turtles, *Chelonia mydas*, exposed to plastic in a frontal
592 area of the SW Atlantic. *Mar. Pollut. Bull.* **78**, 56–62 (2014).
- 593 42 Huzzey, L. M. & Brubaker, J. M. The formation of longitudinal fronts in a coastal plain
594 estuary. *J. Geophys. Res. Oceans* **93**, 1329–1334 (1988).
- 595 43 Nunes, R. & Simpson, J. Axial convergence in a well-mixed estuary. *Estuar. Coast. Shelf
596 Sci.* **20**, 637–649 (1985).
- 597 44 Reeves, A. & Duck, R. Density fronts: Sieves in the estuarine sediment transfer system?
598 *Phys. Chem. Earth Pt B Hydrol. Oceans Atmos.* **26**, 89–92 (2001).
- 599 45 Corlett, W. B. & Geyer, W. R. Frontogenesis at estuarine junctions. *Estuaries Coast* **43**,
600 722–738 (2020).
- 601 46 Bowman, M. J. & Iverson, R. L. in *Oceanic Fronts in Coastal Processes* (ed. Bowman, M.
602 J. & Esaias, W. E.) 87–104 (Springer, 1978).
- 603 47 Largier, J. L. Tidal intrusion fronts. *Estuaries* **15**, 26–39 (1992).
- 604 48 Simpson, J. & Turrell, W. in *Estuarine Variability* (ed. Wolfe, D. A.) 139–152 (Elsevier,
605 1986).
- 606 49 Marmorino, G. & Trump, C. High-resolution measurements made across a tidal intrusion
607 front. *J. Geophys. Res. Oceans* **101**, 25661–25674 (1996).
- 608 50 Horner-Devine, A. R., Hetland, R. D. & MacDonald, D. G. Mixing and transport in coastal
609 river plumes. *Annu. Rev. Fluid Mech.* **47**, 569–594 (2015).
- 610 51 O'Donnell, J., Ackleson, S. G. & Levine, E. R. On the spatial scales of a river plume. *J.
611 Geophys. Res.* **113**, C04017 (2008).
- 612 52 Akan, Ç., McWilliams, J. C., Moghimi, S. & Özkan-Haller, H. T. Frontal dynamics at the
613 edge of the Columbia River plume. *Ocean Model.* **122**, 1–12 (2018).
- 614 53 Giddings, S. N. et al. Frontogenesis and frontal progression of a trapping-generated
615 estuarine convergence front and its influence on mixing and stratification. *Estuaries Coasts*
616 **35**, 665–681 (2012).
- 617 54 van Sebille, E. et al. The physical oceanography of the transport of floating marine debris.
618 *Environ. Res. Lett.* **15**, 023003 (2020).
- 619 55 Cózar, A. et al. Marine litter windrows: A strategic target to understand and manage the
620 ocean plastic pollution. *Front. Mar. Sci.* **8**, 98 (2021).

621 56 Collignon, A. et al. Neustonic microplastic and zooplankton in the North Western
622 Mediterranean Sea. *Mar. Pollut. Bull.* **64**, 861–864 (2012).

623 57 Suaria, G. et al. in *The Handbook of Environmental Chemistry* (ed. Barceló, D. &
624 Kostianoy A. G.) 1–51 (Springer, 2022).

625 58 Brach, L. et al. Anticyclonic eddies increase accumulation of microplastic in the North
626 Atlantic subtropical gyre. *Mar. Pollut. Bull.* **126**, 191–196 (2018).

627 59 Gove, J. M. et al. Prey-size plastics are invading larval fish nurseries. *Proc. Natl. Acad. Sci.*
628 **116**, 24143–24149 (2019).

629 60 Hajbane, S. et al. Coastal garbage patches: Fronts accumulate plastic films at Ashmore
630 Reef Marine Park (Pulau Pasir), Australia. *Front. Mar. Sci.* **8**, 379 (2021).

631 61 Law, K. L. et al. Distribution of surface plastic debris in the eastern Pacific Ocean from an
632 11-year data set. *Environ. Sci. Technol.* **48**, 4732–4738 (2014).

633 62 Isobe, A. et al. A multilevel dataset of microplastic abundance in the world’s upper ocean
634 and the Laurentian Great Lakes. *Microplastics Nanoplastics* **1**, 1–14 (2021).

635 63 Koelmans, A. A., Redondo-Hasselerharm, P. E., Mohamed Nor, N. H. & Kooi, M. Solving
636 the nonalignment of methods and approaches used in microplastic research to consistently
637 characterize risk. *Environ. Sci. Technol.* **54**, 12307–12315 (2020).

638 64 Egger, M., Sulu-Gambari, F. & Lebreton, L. First evidence of plastic fallout from the North
639 Pacific Garbage Patch. *Sci. Rep.* **10**, 1–10 (2020).

640

641 65 Lebreton, L. et al. Evidence that the Great Pacific Garbage Patch is rapidly accumulating
642 plastic. *Sci. Rep.* **8**, 1–15 (2018).

643 66 Cohen, J. H., Internicola, A. M., Mason, R. A. & Kukulka, T. Observations and simulations
644 of microplastic debris in a tide, wind, and freshwater-driven estuarine environment: The
645 Delaware Bay. *Environ. Sci. Technol.* **53**, 14204–14211 (2019).

646 67 Bermúdez, M. et al. Unravelling spatio-temporal patterns of suspended microplastic
647 concentration in the Natura 2000 Guadalquivir estuary (SW Spain): Observations and
648 model simulations. *Mar. Pollut. Bull.* **170**, 112622 (2021).

649 68 Simpson, J. & James, I. in *Baroclinic Processes on Continental Shelves, Volume 3* (ed.
650 Mooers, Ch. N. K.) 63–93 (American Geophysical Union, 1986).

651 69 Andrady, A. L. The plastic in microplastics: A review. *Mar. Pollut. Bull.* **119**, 12–22 (2017).

652 70 Andrady, A., Pandey, K. & Heikkilä, A. Interactive effects of solar UV radiation and
653 climate change on material damage. *Photochem. Photobiol. Sci.* **18**, 804–825 (2019).

654 71 Corcoran, P. L., Biesinger, M. C. & Grifi, M. Plastics and beaches: A degrading
655 relationship. *Mar. Pollut. Bull.* **58**, 80–84 (2009).

656 72 Ter Halle, A. et al. Understanding the fragmentation pattern of marine plastic debris.
657 *Environ. Sci. Technol.* **50**, 5668–5675 (2016).

658 73 Song, Y. K. et al. Combined effects of UV exposure duration and mechanical abrasion on
659 microplastic fragmentation by polymer type. *Environ. Sci. Technol.* **51**, 4368–4376 (2017).

660 74 Andrady, A., Law, K., Donohue, J. & Proskurowski, G. in *MICRO 2016. Fate and Impact
661 of Microplastics in Marine Ecosystems* (ed. Baztan, J., Jorgensen, B., Pahl, S., Thompson,
662 R. C., Vanderlinden, J. P.) 91 (Elsevier, 2017).

663 75 Resmeriță, A.-M. et al. Erosion as a possible mechanism for the decrease of size of plastic
664 pieces floating in oceans. *Mar. Pollut. Bull.* **127**, 387–395 (2018).

665 76 Sekudewicz, I., Dąbrowska, A. M. & Syczewski, M. D. Microplastic pollution in surface
666 water and sediments in the urban section of the Vistula River (Poland). *Sci. Total Environ.*
667 **762**, 143111 (2021).

668 77 Campanale, C. et al. Microplastics and their possible sources: The example of Ofanto river
669 in southeast Italy. *Environ. Pollut.* **258**, 113284 (2020).

670 78 Wang, J. et al. Microplastics in the surface sediments from the Beijiang River littoral zone:
671 Composition, abundance, surface textures and interaction with heavy metals. *Chemosphere*
672 **171**, 248–258 (2017).

673 79 Zhao, S., Zhu, L. & Li, D. Microplastic in three urban estuaries, China. *Environ. Pollut.*
674 **206**, 597–604 (2015).

675 80 Geyer, W., Hill, P. & Kineke, G. The transport, transformation and dispersal of sediment
676 by buoyant coastal flows. *Cont. Shelf Res.* **24**, 927–949 (2004).

677 81 Gregory, J. & O'Melia, C. R. Fundamentals of flocculation. *Crit. Rev. Environ. Sci. Technol.*
678 **19**, 185–230 (1989).

679 82 McCave, I. Size spectra and aggregation of suspended particles in the deep ocean. *Deep*
680 *Sea Res. A. Oceanogr. Res. Pap.* **31**, 329–352 (1984).

681 83 van Leussen, W. in *Physical Processes in Estuaries* (ed. Dronkers, J & van Leussen, W.)
682 347–403 (Springer, 1988).

683 84 Seyvet, O. & Navard, P. Collision-induced dispersion of agglomerate suspensions in a
684 shear flow. *J. Appl. Polym. Sci.* **78**, 1130–1133 (2000).

685 85 Burd, A. B. & Jackson, G. A. Particle aggregation. *Annu. Rev. Mar. Sci.* **1**, 65–90 (2009).

686 86 Efimova, I., Bagaeva, M., Bagaev, A., Kileso, A. & Chubarenko, I. P. Secondary
687 microplastics generation in the sea swash zone with coarse bottom sediments: Laboratory
688 experiments. *Front. Mar. Sci.* **5**, 313 (2018).

689 87 Chubarenko, I., Efimova, I., Bagaeva, M., Bagaev, A. & Isachenko, I. On mechanical
690 fragmentation of single-use plastics in the sea swash zone with different types of bottom
691 sediments: Insights from laboratory experiments. *Mar. Pollut. Bull.* **150**, 110726 (2020).

692 88 Enfrin, M. et al. Release of hazardous nanoplastic contaminants due to microplastics
693 fragmentation under shear stress forces. *J. Hazard. Mater.* **384**, 121393 (2020).

694 89 Edzwald, J. K., Upchurch, J. B. & O'Melia, C. R. Coagulation in estuaries. *Environ. Sci.*
695 *Technol.* **8**, 58–63 (1974).

696 90 Mosley, L. M., Hunter, K. A. & Ducker, W. A. Forces between colloid particles in natural
697 waters. *Environ. Sci. Technol.* **37**, 3303–3308 (2003).

698 91 Sholkovitz, E. Flocculation of dissolved organic and inorganic matter during the mixing of
699 river water and seawater. *Geochim. Cosmochim. Acta* **40**, 831–845 (1976).

700 92 Hunter, K. A. & Leonard, M. W. Colloid stability and aggregation in estuaries: 1.
701 Aggregation kinetics of riverine dissolved iron after mixing with seawater. *Geochim.*
702 *Cosmochim. Acta* **52**, 1123–1130 (1988).

703 93 Claesson, P. M. & Christenson, H. K. Very long range attractive forces between uncharged
704 hydrocarbon and fluorocarbon surfaces in water. *J. Chem. Phys.* **92**, 1650–1655 (1988).

705 94 Israelachvili, J. & Pashley, R. Measurement of the hydrophobic interaction between two
706 hydrophobic surfaces in aqueous electrolyte solutions. *J. Colloid Interface Sci.* **98**, 500–
707 514 (1984).

708 95 Geesey, G. Microbial exopolymers: Ecological and economic considerations. *ASM News*
709 **48**, 9–14 (1982).

710 96 Alldredge, A. L. & Silver, M. W. Characteristics, dynamics and significance of marine
711 snow. *Prog. Oceanogr.* **20**, 41–82 (1988).

712 97 Verdugo, P. Marine microgels. *Ann. Rev. Mar. Sci.* **4**, 375–400 (2012).

713 98 Engel, A. The role of transparent exopolymer particles (TEP) in the increase in apparent
714 particle stickiness (α) during the decline of a diatom bloom. *J. Plankton Res.* **22**, 485–497
715 (2000).

716 99 Mopper, K., Ramana, K. S. & Drapeau, D. T. The role of surface-active carbohydrates in
717 the flocculation of a diatom bloom in a mesocosm. *Deep-Sea Res. Part II Top. Stud.*
718 *Oceanogr.* **42**, 47–73 (1995).

719 100 Decho, A. W. & Gutierrez, T. Microbial extracellular polymeric substances (EPSs) in
720 ocean systems. *Front. Microbiol.* **8**, 922 (2017).

721 101 Kiørboe, T. & Hansen, J. L. Phytoplankton aggregate formation: Observations of patterns
722 and mechanisms of cell sticking and the significance of exopolymeric material. *J. Plankton*
723 *Res.* **15**, 993–1018 (1993).

724 102 Passow, U. Transparent exopolymer particles (TEP) in aquatic environments. *Prog.*
725 *Oceanogr.* **55**, 287–333 (2002).

726 103 Michels, J., Stippkugel, A., Lenz, M., Wirtz, K. & Engel, A. Rapid aggregation of biofilm-
727 covered microplastics with marine biogenic particles. *Proc. Royal Soc. B* **285**, 20181203
728 (2018).

729 104 Galgani, L. et al. Microplastics increase the marine production of particulate forms of
730 organic matter. *Environ. Res. Lett.* **14**, 124085 (2019).

731 105 Long, M. et al. Interactions between microplastics and phytoplankton aggregates: Impact
732 on their respective fates. *Mar. Chem.* **175**, 39–46 (2015).

733 106 Mari, X. et al. Aggregation dynamics along a salinity gradient in the Bach Dang estuary,
734 North Vietnam. *Estuar. Coast. Shelf Sci.* **96**, 151–158 (2012).

735 107 Beauvais, S., Pedrotti, M., Egge, J., Iversen, K. & Marrasé, C. Effects of turbulence on
736 TEP dynamics under contrasting nutrient conditions: Implications for aggregation and
737 sedimentation processes. *Mar. Ecol. Prog. Ser.* **323**, 47–57 (2006).

738 108 Thornton, D. C. Phytoplankton mucilage production in coastal waters: A dispersal
739 mechanism in a front dominated system? *Ethol. Ecol. Evol.* **11**, 179–185 (1999).

740 109 Degobbi, D. et al. Changes in the northern Adriatic ecosystem and the hypertrophic
741 appearance of gelatinous aggregates. *Sci. Total Environ.* **165**, 43–58 (1995).

742 110 Zhao, S., Ward, J. E., Danley, M. & Mincer, T. J. Field-based evidence for microplastic in
743 marine aggregates and mussels: Implications for trophic transfer. *Environ. Sci. Technol.*
744 **52**, 11038–11048 (2018).

745 111 Ward, J. E. & Kach, D. J. Marine aggregates facilitate ingestion of nanoparticles by
746 suspension-feeding bivalves. *Mar. Environ. Res.* **68**, 137–142 (2009).

747 112 Wotton, R. S. & Malmqvist, B. Feces in aquatic ecosystems: Feeding animals transform
748 organic matter into fecal pellets, which sink or are transported horizontally by currents;
749 these fluxes relocate organic matter in aquatic ecosystems. *BioScience* **51**, 537–544 (2001).

750 113 Arlinghaus, P., Zhang, W., Wrede, A., Schrum, C. & Neumann, A. Impact of benthos on
751 morphodynamics from a modeling perspective. *Earth Sci. Rev.* 103803 (2021).

752 114 Bhaskar, P. & Bhosle, N. B. Microbial extracellular polymeric substances in marine
753 biogeochemical processes. *Current Science*, 45–53 (2005).

754 115 Dame, R. & Allen, D. Between estuaries and the sea. *J. Exp. Mar. Biol. Ecol.* **200**, 169–
755 185 (1996).

756 116 Taylor, J. R. Accumulation and subduction of buoyant material at submesoscale fronts. *J.*
757 *Phys. Oceanogr.* **48**, 1233–1241 (2018).

758 117 Brunner, K., Kukulka, T., Proskurowski, G. & Law, K. L. Passive buoyant tracers in the
759 ocean surface boundary layer: 2. Observations and simulations of microplastic marine
760 debris. *J. Geophys. Res. Oceans* **120**, 7559–7573 (2015).

761 118 Porter, A., Lyons, B. P., Galloway, T. S. & Lewis, C. Role of marine snows in microplastic
762 fate and bioavailability. *Environ. Sci. Technol.* **52**, 7111–7119 (2018).

763 119 Zhao, S., Danley, M., Ward, J. E., Li, D. & Mincer, T. J. An approach for extraction,
764 characterization and quantitation of microplastic in natural marine snow using Raman
765 microscopy. *Anal. Methods* **9**, 1470–1478 (2017).

766 120 Cole, M. et al. Microplastics alter the properties and sinking rates of zooplankton faecal
767 pellets. *Environ. Sci. Technol.* **50**, 3239–3246 (2016).

768 121 Brahney, J., Hallerud, M., Heim, E., Hahnenberger, M. & Sukumaran, S. Plastic rain in
769 protected areas of the United States. *Science* **368**, 1257–1260 (2020).

770 122 Bergmann, M. et al. White and wonderful? Microplastics prevail in snow from the Alps to
771 the Arctic. *Sci. Adv.* **5**, eaax1157 (2019).

772 123 Allen, S. et al. Atmospheric transport and deposition of microplastics in a remote mountain
773 catchment. *Nat. Geosci.* **12**, 339–344 (2019).

774 124 Dris, R., Gasperi, J., Saad, M., Mirande, C. & Tassin, B. Synthetic fibers in atmospheric
775 fallout: A source of microplastics in the environment? *Mar. Pollut. Bull.* **104**, 290–293
776 (2016).

777 125 Rochman, C. M. & Hoellein, T. The global odyssey of plastic pollution. *Science* **368**, 1184–
778 1185 (2020).

779 126 Allen, S. et al. Examination of the ocean as a source for atmospheric microplastics. *PloS*
780 *one* **15**, e0232746 (2020).

781 127 Trainic, M. et al. Airborne microplastic particles detected in the remote marine atmosphere.
782 *Commun. Earth Environ.* **1**, 1–9 (2020).

783 128 Brahney, J. et al. Constraining the atmospheric limb of the plastic cycle. *Proc. Natl. Acad.*
784 *Sci.* **118** (2021).

785 129 Kudela, R. M. et al. Multiple trophic levels fueled by recirculation in the Columbia River
786 plume. *Geophys. Res. Lett.* **37** (2010).

787 130 Zamon, J. E., Phillips, E. M. & Guy, T. J. Marine bird aggregations associated with the
788 tidally-driven plume and plume fronts of the Columbia River. *Deep Sea Res. Part II Top.*
789 *Stud. Oceanogr.* **107**, 85–95 (2014).

790 131 Scotti, A. & Pineda, J. Plankton accumulation and transport in propagating nonlinear
791 internal fronts. *J. Mar. Res.* **65**, 117–145 (2007).

792 132 Choy, E. S., Kimpe, L. E., Mallory, M. L., Smol, J. P. & Blais, J. M. Contamination of an
793 arctic terrestrial food web with marine-derived persistent organic pollutants transported by
794 breeding seabirds. *Environ. Pollut.* **158**, 3431–3438 (2010).

795 133 Ewald, G., Larsson, P., Linge, H., Okla, L. & Szarzi, N. Biotransport of organic pollutants
796 to an inland Alaska lake by migrating sockeye salmon (*Oncorhynchus nerka*). *Arctic*, 40–
797 47 (1998).

798 134 Montory, M. et al. Biotransport of persistent organic pollutants in the southern Hemisphere
799 by invasive Chinook salmon (*Oncorhynchus tshawytscha*) in the rivers of northern Chilean
800 Patagonia, a UNESCO biosphere reserve. *Environ. Int.* **142**, 105803 (2020).

801 135 De Robertis, A. et al. Columbia River plume fronts. II. Distribution, abundance, and
802 feeding ecology of juvenile salmon. *Mar. Ecol. Prog. Ser.* **299**, 33–44 (2005).

803 136 Lange, M. & van Sebille, E. Parcels v0. 9: Prototyping a Lagrangian ocean analysis
804 framework for the petascale age. *Geosci. Model Dev.* **10**, 4175–4186 (2017).

805 137 van Sebille, E. et al. Lagrangian ocean analysis: Fundamentals and practices. *Ocean Model.*
806 **121**, 49–75 (2018).

807 138 Onink, V., van Sebille, E. & Laufkötter, C. Empirical Lagrangian parametrization for wind-
808 driven mixing of buoyant particles at the ocean surface. *Geosci. Model Dev.* **15**, 1995–
809 2012 (2022).

810 139 Genc, A. N., Vural, N. & Balas, L. Modeling transport of microplastics in enclosed coastal
811 waters: A case study in the Fethiye Inner Bay. *Mar. Pollut. Bull.* **150**, 110747 (2020).

812 140 Jalón-Rojas, I., Wang, X. H. & Fredj, E. A 3D numerical model to track marine plastic
813 debris (TrackMPD): Sensitivity of microplastic trajectories and fates to particle dynamical
814 properties and physical processes. *Mar. Pollut. Bull.* **141**, 256–272 (2019).

815

816 141 Sousa, M. C. et al. Modelling the distribution of microplastics released by wastewater
817 treatment plants in Ria de Vigo (NW Iberian Peninsula). *Mar. Pollut. Bull.* **166**, 112227
818 (2021).

819 142 López, A. G., Najjar, R. G., Friedrichs, M. A., Hickner, M. A. & Wardrop, D. H.
820 Estuaries as Filters for Riverine Microplastics: Simulations in a Large, Coastal-Plain
821 Estuary. *Front. Environ. Sci.* **26** (2021).

822 143 Mountford, A. & Morales Maqueda, M. Eulerian Modeling of the three-dimensional
823 distribution of seven popular microplastic types in the global ocean. *J. Geophys. Res.*
824 *Oceans* **124**, 8558–8573 (2019).

825 144 Fischer, R. et al. Modelling submerged biofouled microplastics and their vertical
826 trajectories. *Biogeosciences* **19**, 2211–2234 (2022).

827 145 Kaandorp, M. L., Dijkstra, H. A. & van Sebille, E. Modelling size distributions of marine
828 plastics under the influence of continuous cascading fragmentation. *Environ. Res. Lett.*
829 **16**, 054075 (2021).

830 146 Sterl, M. F., Delandmeter, P. & van Sebille, E. Influence of barotropic tidal currents on
831 transport and accumulation of floating microplastics in the global open ocean. *J.*
832 *Geophys. Res. Oceans* **125**, e2019JC015583 (2020).

833 147 Wichmann, D., Delandmeter, P. & van Sebille, E. Influence of near-surface currents on
834 the global dispersal of marine microplastic. *J. Geophys. Res. Oceans* **124**, 6086–6096
835 (2019).

836 148 Eriksen, M. et al. Plastic pollution in the world's oceans: More than 5 trillion plastic
837 pieces weighing over 250,000 tons afloat at sea. *PLoS One* **9**, e111913 (2014).

838 149 Cózar, A. et al. Plastic debris in the open ocean. *Proc. Natl. Acad. Sci.* **111**, 10239–10244
839 (2014).

840 150 Kaandorp, M. L., Dijkstra, H. A. & van Sebille, E. Closing the Mediterranean marine
841 floating plastic mass budget: Inverse modeling of sources and sinks. *Environ. Sci.*
842 *Technol.* **54**, 11980–11989 (2020).

843 151 Cloux, S. et al. Validation of a Lagrangian model for large-scale macroplastic tracer
844 transport using mussel-peg in NW Spain (Ría de Arousa). *Sci. Total Environ.* **822**,
845 153338 (2022).

- 846 152 Cheng, M. L. et al. A baseline for microplastic particle occurrence and distribution in Great
847 Bay Estuary. *Mar. Pollut. Bull.* **170**, 112653 (2021).
- 848 153 Koelmans, A. A., Kooi, M., Law, K. L. & van Sebille, E. All is not lost: Deriving a top-
849 down mass budget of plastic at sea. *Environ. Res. Lett.* **12**, 114028 (2017).
- 850 154 Kooi, M., van Nes, E. H., Scheffer, M. & Koelmans, A. A. Ups and downs in the ocean:
851 Effects of biofouling on vertical transport of microplastics. *Environ. Sci. Technol.* **51**,
852 7963–7971 (2017).
- 853 155 Isobe, A., Iwasaki, S., Uchida, K. & Tokai, T. Abundance of non-conservative
854 microplastics in the upper ocean from 1957 to 2066. *Nat. Commun.* **10**, 1–13 (2019).
- 855 156 Karati, K. K. et al. River plume fronts and their implications for the biological production
856 of the Bay of Bengal, Indian Ocean. *Mar. Ecol. Prog. Ser.* **597**, 79–98 (2018).
- 857 157 Mohammed, A. in *New insights into toxicity and drug testing* (ed. Gowder S.) 49–62
858 (Intech, 2013).
- 859 158 Steer, M., Cole, M., Thompson, R. C. & Lindeque, P. K. Microplastic ingestion in fish
860 larvae in the western English Channel. *Environ. Pollut.* **226**, 250–259 (2017).
- 861 159 Taha, Z. D., Amin, R. M., Anuar, S. T., Nasser, A. A. A. & Sohaimi, E. S. Microplastics
862 in seawater and zooplankton: A case study from Terengganu estuary and offshore waters,
863 Malaysia. *Sci. Total Environ.* **786**, 147466 (2021).
- 864 160 Desforges, J.-P. W., Galbraith, M. & Ross, P. S. Ingestion of microplastics by
865 zooplankton in the Northeast Pacific Ocean. *Arch. Environ. Contam. Toxicol.* **69**, 320–
866 330 (2015).
- 867 161 Jaafar, N. et al. Occurrence, distribution and characteristics of microplastics in
868 gastrointestinal tract and gills of commercial marine fish from Malaysia. *Sci. Total*
869 *Environ.* **799**, 149457 (2021).
- 870 162 Wicczorek, A. M., Croot, P. L., Lombard, F., Sheahan, J. N. & Doyle, T. K. Microplastic
871 ingestion by gelatinous zooplankton may lower efficiency of the biological pump.
872 *Environ. Sci. Technol.* **53**, 5387–5395 (2019).
- 873 163 Lusher, A., Hollman, P. & Mendoza-Hill, J. *Microplastics in fisheries and aquaculture:*
874 *status of knowledge on their occurrence and implications for aquatic organisms and food*
875 *safety*. (FAO, 2017).
- 876 164 Gigault, J. et al. Nanoplastics are neither microplastics nor engineered nanoparticles. *Nat.*
877 *Nanotechnol.* **16**, 501–507 (2021).
- 878 165 Xu, J. et al. Unpalatable plastic: Efficient taste discrimination of microplastics in
879 planktonic copepods. *Environ. Sci. Technol.* **56**, 6455–6465 (2022).
- 880 166 Cole, M. et al. Effects of nylon microplastic on feeding, lipid accumulation, and moulting
881 in a coldwater copepod. *Environ. Sci. Technol.* **53**, 7075–7082 (2019).
- 882 167 Botterell, Z. L. et al. Bioavailability of microplastics to marine zooplankton: Effect of
883 shape and infochemicals. *Environ. Sci. Technol.* **54**, 12024–12033 (2020).
- 884 168 Savoca, M. S., Machovsky-Capuska, G. E., Andrades, R. & Santos, R. G. Plastic
885 ingestion: Understanding causes and impacts. *Front. Environ. Sci.*, 599 (2022).
- 886 169 Vroom, R. J., Koelmans, A. A., Besseling, E. & Halsband, C. Aging of microplastics
887 promotes their ingestion by marine zooplankton. *Environ. Pollut.* **231**, 987–996 (2017).
- 888 170 Ward, J. E. & Kach, D. J. Marine aggregates facilitate ingestion of nanoparticles by
889 suspension-feeding bivalves. *Mar. Environ. Res.* **68**, 137–142 (2009).

- 890 171 Acha, E. M., Piola, A., Iribarne, O. & Mianzan, H. in *Ecological processes at marine*
891 *fronts: oases in the ocean*. (Ed. Acha, E. M., Piola, A., Iribarne, O. & Mianzan, H.) 13–
892 32 (Springer, 2015).
- 893 172 Suhrhoff, T. J. & Scholz-Böttcher, B. M. Qualitative impact of salinity, UV radiation and
894 turbulence on leaching of organic plastic additives from four common plastics—A lab
895 experiment. *Mar. Pollut. Bull.* **102**, 84–94 (2016).
- 896 173 Romera-Castillo, C., Pinto, M., Langer, T. M., Álvarez-Salgado, X. A. & Herndl, G. J.
897 Dissolved organic carbon leaching from plastics stimulates microbial activity in the
898 ocean. *Nat. Commun.* **9**, 1–7 (2018).
- 899 174 Zhu, L., Zhao, S., Bittar, T. B., Stubbins, A. & Li, D. Photochemical dissolution of
900 buoyant microplastics to dissolved organic carbon: rates and microbial impacts. *J.*
901 *Hazard. Mater.* **383**, 121065 (2020).
- 902 175 Groh, K. J. et al. Overview of known plastic packaging-associated chemicals and their
903 hazards. *Sci. Total Environ.* **651**, 3253–3268 (2019).
- 904 176 Seeley, M. E., Song, B., Passie, R. & Hale, R. C. Microplastics affect sedimentary
905 microbial communities and nitrogen cycling. *Nat. Commun.* **11**, 1–10 (2020).
- 906 177 Wei, W. et al. Polyvinyl chloride microplastics affect methane production from the
907 anaerobic digestion of waste activated sludge through leaching toxic bisphenol-A.
908 *Environ. Sci. Technol.* **53**, 2509–2517 (2019).
- 909 178 Kvale, K., Prowe, A., Chien, C.-T., Landolfi, A. & Oschlies, A. Zooplankton grazing of
910 microplastic can accelerate global loss of ocean oxygen. *Nat. Commun.* **12**, 1–8 (2021).
- 911 179 Zobell, C. E. The effect of solid surfaces upon bacterial activity. *J. Bacteriol.* **46**, 39–56
912 (1943).
- 913 180 Galgani, L. & Loiseau, S. A. Plastic accumulation in the sea surface microlayer: An
914 experiment-based perspective for future studies. *Geosciences* **9**, 66 (2019).
- 915 181 Lebreton, L. C. et al. River plastic emissions to the world’s oceans. *Nat. Commun.* **8**, 1–
916 10 (2017).
- 917 182 Schmidt, C., Krauth, T. & Wagner, S. Export of plastic debris by rivers into the sea.
918 *Environ. Sci. Technol.* **51**, 12246–12253 (2017).
- 919 183 van Emmerik, T. & Schwarz, A. Plastic debris in rivers. *Wiley Interdiscip. Rev. Water* **7**,
920 e1398 (2019).
- 921 184 Haberstroh, C. J., Arias, M. E., Yin, Z. & Wang, M. C. Effects of hydrodynamics on the
922 cross-sectional distribution and transport of plastic in an urban coastal river. *Water*
923 *Environ. Res.* **93**, 186–200 (2021).
- 924 185 Borrelle, S. B. et al. Opinion: Why we need an international agreement on marine plastic
925 pollution. *Proc. Natl. Acad. Sci.* **114**, 9994–9997 (2017).
- 926 186 Haberstroh, C. J., Arias, M. E., Yin, Z., Sok, T. & Wang, M. C. Plastic transport in a
927 complex confluence of the Mekong River in Cambodia. *Environ. Res. Lett.* **16**, 095009
928 (2021).
- 929 187 Schreyers, L. et al. Plastic plants: The role of water hyacinths in plastic transport in
930 tropical rivers. *Front. Environ. Sci.* **9**, 177 (2021).
- 931 188 van Emmerik, T., Loozen, M., van Oeveren, K., Buschman, F. & Prinsen, G. Riverine
932 plastic emission from Jakarta into the ocean. *Environ. Res. Lett.* **14**, 084033 (2019).
- 933 189 van Emmerik, T., Strady, E., Kieu-Le, T.-C., Nguyen, L. & Gratiot, N. Seasonality of
934 riverine macroplastic transport. *Sci. Rep.* **9**, 1–9 (2019).

- 935 190 van Calcar, C. & van Emmerik, T. Abundance of plastic debris across European and
936 Asian rivers. *Environ. Res. Lett.* **14**, 124051 (2019).
- 937 191 Gasperi, J., Dris, R., Bonin, T., Rocher, V. & Tassin, B. Assessment of floating plastic
938 debris in surface water along the Seine River. *Environ. Pollut.* **195**, 163–166 (2014).
- 939 192 Lindquist, A. Baltimore’s Mr. trash wheel. *J. Ocean Technol.* **11**, 28–35 (2016).
- 940 193 Kilcher, L. F. & Nash, J. D. Structure and dynamics of the Columbia River tidal plume
941 front. *J. Geophys. Res. Oceans* **115**, C05S90 (2010).
- 942 194 Martin, C. et al. Use of unmanned aerial vehicles for efficient beach litter monitoring.
943 *Mar. Pollut. Bull.* **131**, 662–673 (2018).
- 944 195 Geraeds, M., van Emmerik, T., de Vries, R. & Bin Ab Razak, M. S. Riverine plastic litter
945 monitoring using unmanned aerial vehicles (UAVs). *Remote Sens.* **11**, 2045 (2019).
- 946 196 Eggleston, D. B., Armstrong, D. A., Elis, W. E. & Patton, W. S. Estuarine fronts as
947 conduits for larval transport: Hydrodynamics and spatial distribution of Dungeness crab
948 postlarvae. *Mar. Ecol. Prog. Ser.* **164**, 73–82 (1998).
- 949 197 Sherman, P. & van Sebille, E. Modeling marine surface microplastic transport to assess
950 optimal removal locations. *Environ. Res. Lett.* **11**, 014006 (2016).
- 951 198 Mellink, Y., van Emmerik, T., Kooi, M., Laufkötter, C. & Niemann, H. The plastic
952 pathfinder: A macroplastic transport and fate model for terrestrial environments. Preprint
953 at Earth ArXiv [https://doi.org/ 10.31223/X5303G](https://doi.org/10.31223/X5303G) (2022).
- 954 199 Tramoy, R. et al. Transfer dynamics of macroplastics in estuaries—New insights from the
955 Seine estuary: Part 2. Short-term dynamics based on GPS-trackers. *Mar. Pollut. Bull.*
956 **160**, 111566 (2020).
- 957 200 Li, C. Axial convergence fronts in a barotropic tidal inlet—Sand Shoal Inlet, VA. *Cont.*
958 *Shelf Res.* **22**, 2633–2653 (2002).
- 959 201 Nash, J. D. & Moum, J. N. River plumes as a source of large-amplitude internal waves in
960 the coastal ocean. *Nature* **437**, 400–403 (2005).
- 961 202 Mazzini, P. L. & Chant, R. J. Two-dimensional circulation and mixing in the far field of a
962 surface-advected river plume. *J. Geophys. Res. Oceans* **121**, 3757–3776 (2016).
- 963 203 Macklin, J. T., Ferrier, G., Neill, S. & Folkard, G. Alongtrack interferometry (ATI)
964 observations of currents and fronts in the Tay estuary, Scotland. *EARSeL eProceedings* **3**,
965 179 (2004).
- 966 204 O’Melia, C. R. ES&T features: Aquasols: The behavior of small particles in aquatic
967 systems. *Environ. Sci. Technol.* **14**, 1052–1060 (1980).

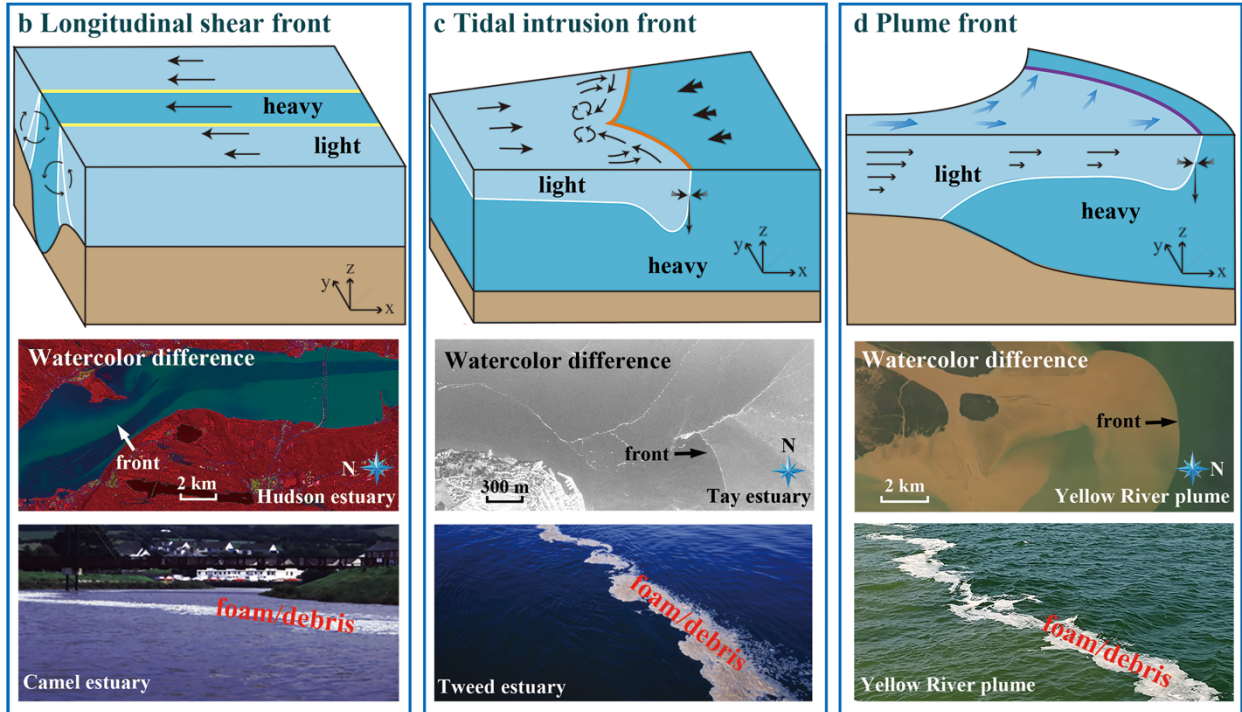
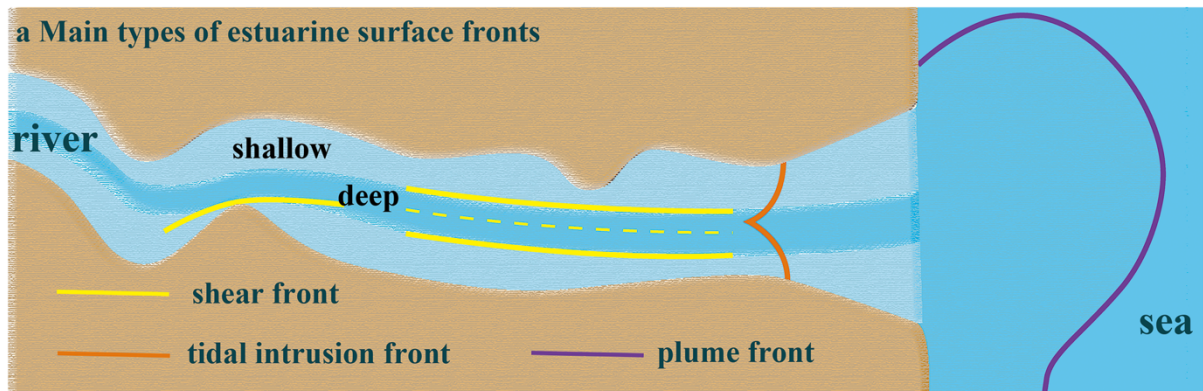
968
969 **Acknowledgements** The authors thank X. Li for her assistance with the illustration in FIGS. 2 and
970 3. The funding support was provided through the Asia-Pacific Network Project (No: CRRP2021-
971 08MY-Zhao) to T.W., R.M.A. and S.Z. This study was also supported by the National Natural
972 Science Foundations of China (42076006 and 41806137), and from the European Union’s Horizon
973 2020 research and innovation programme under the Marie Skłodowska-Curie grant agreement
974 PLOCEAN No 882682 as support of L.G., International Partnership Research Grant, UMT (55379)
975 to R.M.A., and National Research Foundation Singapore through the Marine Environmental.

976 **Competing interests** The authors declare no competing interests.

977 **Author contributions** S.Z was instrumental in initiating this paper. T.W. and S.Z co-led the design
978 and writing of the article and contributed equally to this article. All co-authors provided input on

1003 of magnitude larger than the maximum value of microplastics in the Great Pacific Garbage Patch
 1004 (GPGP, the red diamond)⁶⁴.

1005
 1006
 1007
 1008
 1009
 1010
 1011
 1012
 1013
 1014

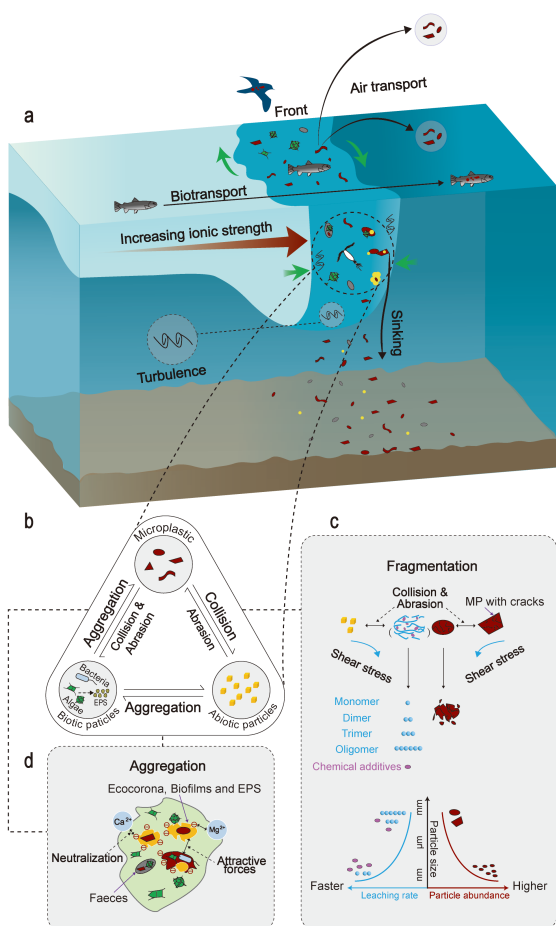


1015
 1016
 1017
 1018

Fig.2 | Schematic diagrams of the main types of estuarine surface fronts and some examples that show their features of apparent watercolor difference and accumulation of foam and

1019
1020
1021
1022
1023
1024
1025
1026
1027
1028
1029
1030

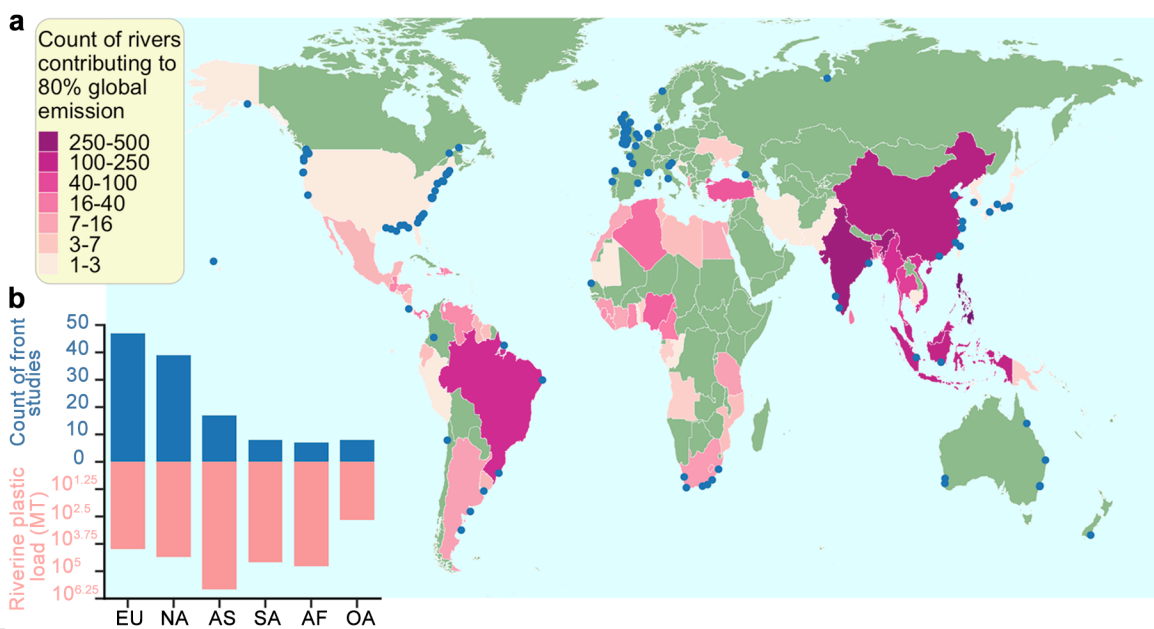
debris. a | Schematic diagram of the locations where the three types of estuarine fronts preferably occur. **b** | Longitudinal front induced by the transverse shear of tidal velocity. **c** | Tidal intrusion front formed when denser coastal waters plunge beneath lighter estuarine waters during a flood tide. **d** | Plume front formed when riverine freshwater of riverine origin spreads over the coastal water. Watercolor images of the Hudson estuary and Yellow River plume are obtained from the Landsat satellite. Watercolor image of the Tay estuary is adapted from REF²⁰³. Photograph of the foam and debris lines in the Yellow River plume is taken by Tao Wang in August, 2021. Photographs of the foam and debris lines in the Camel estuary and Tweed estuary are adapted from REF¹³.



1031
1032
1033
1034
1035
1036
1037
1038
1039
1040

FIG | 3 Transport and transformation of microplastics in the frontal zone. a | The concurrent accumulation of organisms and microplastics due to the combination of passive convergent transport and bio-behavioral movement in response to frontal structures¹⁹. The convergence of phytoplankton biomass ultimately attracts animals of higher trophic levels. These animals interact with microplastics and subsequently lead to plastic redistribution. Microplastics and fibers trapped in mucilaginous foams along the fronts could be lofted into the air by breaking waves and winds, which facilitate microplastics atmospheric transport^{123,126-128}. The strong downwelling currents and turbulence at fronts are able to subduct microplastics into the water column^{116,117}. **b** | Interactions between microplastics and other particles (both biotic and abiotic particles) in frontal systems. **c** |

1041 The processes of microplastic fragmentation. The enhanced collision frequency of particles in
 1042 frontal systems results in the accelerated disintegration of microplastics through the detachment
 1043 mechanism⁸⁴. Simultaneously, the leaching of plastic-derived carbon (for example, monomer,
 1044 trimer and oligomer) and chemical additives could also be enhanced by plastic fragmentation and
 1045 strong turbulence occurring at fronts^{164,172}. The abundances of secondary microplastics and
 1046 leaching rates of chemicals increase exponentially with the decrease of particle size¹⁶⁴. **d** |
 1047 Microplastics aggregation with non-living and living particles at fronts. Besides the increased
 1048 collision rates that bring particles together (BOX 1), the increased cations toward the sea^{11,89} and
 1049 the hydrophobicity of plastic particles⁸¹ facilitate the attractions between particles. Additionally,
 1050 the expectedly high concentrations of extracellular polymeric substances (EPS) exuded by the
 1051 microorganisms, can glue these particles together and enhance aggregation^{98,103,105}.
 1052



1053 **Fig.4 | Global research of estuarine fronts and riverine plastic flux. a** | The global map with
 1054 each country shaded according to the number out of 1656 rivers for 80% of the total plastic flux
 1055 to the ocean. The annual plastic emission into the ocean emitted by 1656 rivers in total is ~0.8
 1056 million metric tons (MT)⁷. Countries not included any of the 1656 rivers are shaded green. Blue
 1057 dots indicate the locations of estuaries (n=126) where the fronts have been studied in 172
 1058 publications (Supplementary Table 2). **b** | The number of estuaries where estuarine fronts are
 1059 reported (n=126; blue bars) and annual plastic emission into the ocean emitted by 1656 rivers (pink
 1060 bars) in each continent (Europe, EU; North American, NA; Asia, AS; South America, SA; Africa,
 1061 AF; Oceania, OA). Currently, research of estuarine fronts is mainly conducted in Europe and North
 1062 America (blue bars). Annually, the largest contributing continent is Asia with 1278 rivers emitting
 1063 60,542 MT, followed by Africa with 60,542 MT through 145 rivers, South America with 39,572
 1064 MT through 108 rivers, North America with 22,468 MT through 85 rivers, Europe with 9436 MT
 1065 through 46 rivers, and Oceania with 445 MT through 2 rivers. The striking mismatch between the
 1066 geographical location of studies on estuarine fronts and main rivers responsible for plastic loads
 1067 into the ocean suggests that urgent efforts on understanding processes in estuarine front are
 1068 required for the mitigation of riverine plastic debris in ‘hotspots’ like the Asian and African
 1069 continents.
 1070
 1071

Box 1 | Encounter kernel rate of particles in aquatic systems

Collision of particles in turbulent flow fields is a physical process bringing particles into contact with each other⁸⁴. The encounter kernel rate of particles determines the rate of collision between particles, which generally depends on three transport processes^{81,85}, including Brownian diffusion (β_{Br}), fluid shear (β_{sh}) and differential sedimentation (β_{ds}). Brownian diffusion is the random motion that brings particles together through thermal effects. Fluid shear in which velocity gradients occur, induces interparticle contact among the particles carried by the fluid. Collision by differential sedimentation occurs when two particles have different settling velocities due to the gravity effects²⁰⁴. The total encounter kernel rate (β_{ij}) between two particles of size i and j is their sum⁴:

$$\beta_{ij} = \beta_{Br}(i, j) + \beta_{sh}(i, j) + \beta_{ds}(i, j)$$

$$\beta_{Br}(i, j) = \frac{2kT(r_i+r_j)^2}{3\mu(r_i r_j)}; \beta_{sh}(i, j) = 1.3^2 \sqrt{\varepsilon/\nu} \cdot (r_i + r_j)^3; \beta_{ds}(i, j) = \pi(r_i + r_j)^2 |\omega_i - \omega_j|$$

where k is Boltzman constant; T is the absolute temperature; μ and ν are the dynamic and kinematic viscosities, respectively; ε is the turbulent kinetic energy dissipation rate, and ω_i is the settling velocity of a particle with radius r_i .

These encounter kernel rates by three mechanisms vary with particle sizes. The kernel rate by Brownian motion plays a minor role in bringing particles ($>1 \mu\text{m}$) together⁸¹, thus it is not included to explain the collision rate of microplastics. As particle size increases, collisions arising from shear (either turbulent or laminar) and differential sedimentation, become more important⁸². Shear-induced collision is known to be stronger than other transport mechanisms⁸³, and was demonstrated to be important in the high particle concentration and high shear environment of the boundary layer⁸². Therefore, strong turbulent energy and high particle load at estuarine fronts can facilitate higher collision rates between plastic and other particles, leading to particle aggregation and/or plastic fragmentation through the surface ablation mode^{69,70} (FIG. 3b).